ECEE2026
18th European Conference on Earthquake Engineering

Seismic Vulnerability Database for Earthquake-induced Embodied Carbon in Europe

Karim Aljawhari[1,2], Martina Caruso[2], Al Mouayed Bellah Nafeh[1], Vitor Silva[1,3]

1- Global Earthquake Model (GEM) Foundation, Via Ferrata 1, Pavia, 27100, Italy
2- University College London (UCL), Gower Street, London, WC1E 6BT, United Kingdom
3- Universidade de Aveiro, 3810-193, Aveiro, Portugal

Corresponding Author's E-mail: karim.aljawhari@globalquakemodel.org

Abstract

The growing emphasis on sustainability in the built environment highlights the need to explicitly address the environmental impacts of earthquake damage in seismic risk assessments. While previous studies have focused on individual components or limited building types, embodied-carbon vulnerability functions applicable at national and global scales remain largely unavailable. This study develops a database of structural vulnerability functions for earthquake-induced embodied carbon for Europe. This database is created within the scope of the Global Vulnerability Model supported by the Global Earthquake Model (GEM) Foundation. The proposed functions quantify the carbon footprint associated with seismic damage to structural components, enabling consistent life-cycle impact assessment within large-scale seismic risk frameworks. Vulnerability functions are derived by first developing damage-to-carbon ratios that link global damage states (slight, moderate, extensive, and complete) to the corresponding embodied carbon, expressed as a fraction of building replacement value. These ratios are obtained by analysing the emissions associated with repair actions for the main components of reinforced concrete, steel, timber, and masonry buildings. The resulting open-access database of embodied-carbon vulnerability functions, distributed via GitHub, provides a scalable tool for integrating resilience and sustainability objectives in regional and global decision-making.

Keywords: embodied carbon, vulnerability, seismic risk, environmental impacts, fragility.

1- INTRODUCTION

Earthquakes can cause substantial damage to the built environment, generating not only economic losses, but also considerable environmental impacts due to post-disaster repair and reconstruction activities, as shown by multiple past events [1,2]. As the construction sector is a major contributor to global greenhouse gas emissions [3] and the resulting climate change, there is growing interest in quantifying the emissions associated with earthquake-induced damage as an additional source of embodied carbon. This requires methods that can translate physical damage into carbon footprint with sufficient resolution and consistency across different building classes and geographic contexts.

Recent works have begun to establish the basis for assessing earthquake-induced environmental impacts by integrating them in typical building life-cycle analyses [4,5] or even use them in decision-making related to the design and selection of building rehabilitation strategies [6–8]. Despite this progress, explicit quantification of embodied carbon from seismic damage is still limited, especially for regional applications. Studies have typically focused on individual structural and non-structural components [9,10] or on a few building classes, such as reinforced concrete frames [9,11] that are not representative of regional construction diversity.

The first large-scale attempt to evaluate seismic risk in terms of embodied carbon was presented by Caruso et al. [12], who considered Europe as a test bed. This constituted an important step toward continental-scale environmental risk quantification. However, a key limitation of this study is that it did not use carbon-specific seismic vulnerability functions, so the environmental losses were estimated by assuming that repair cost ratios (repair cost normalised by replacement cost) could be used as a proxy for embodied carbon ratios (embodied carbon of seismic damage normalised by replacement carbon). While practical, this assumption

implies that economic vulnerability is equivalent to carbon vulnerability, despite the fact that repair costs and embodied carbon are driven by different material and labour contributions.

The current work tackles the above research gaps by developing a database for carbon-specific seismic vulnerability functions for Europe, enabling a more physically meaningful representation of earthquake environmental consequences across the entire building stock. These functions are primarily based on identifying repair activities required to reinstate a building's structural components to their original condition when they sustain various levels of damage (also called damage states, DSs). This is followed by estimating material types and quantities needed for each repair activity, which are eventually multiplied by region-specific embodied carbon factors (ECFs), which express greenhouse gas emissions in kilograms of carbon dioxide equivalent ($kgCO_2e$) per unit quantity of material.

2- METHODOLOGY

This study develops a database of seismic vulnerability functions to quantify the environmental loss associated with structural damage, expressed in terms of embodied carbon, as a function of ground-shaking intensity. These functions can be generated using Eq. **Error! Reference source not found.**), where $CR|IM$ is the embodied carbon ratio (repair-related embodied carbon normalised by the building total replacement embodied carbon), conditional on a given intensity measure (IM) level. $P(DS = DS_i \mid IM)$ represents the probability that the building is in the i-th damage state (DS_i) at that IM level. DCR_{DS_i} is the carbon-specific consequence model, also referred to as the damage-to-carbon ratio, which converts each damage state into an embodied carbon ratio (i.e., the embodied carbon required to repair DS_i, normalised by the building replacement carbon).

$$\boldsymbol{CR|IM} = \sum_{\boldsymbol{i=1}}^{\boldsymbol{n}} \boldsymbol{DCR_{DSi}} \cdot \boldsymbol{P(DS = DSi|IM)} \tag{1}$$

The damage-state probabilities in Eq. **Error! Reference source not found.**), $P(DS = DS_i \mid IM)$, are derived from fragility functions, which describe the probability of exceeding different DSs for a given IM level. Four damage states are considered in this study: slight damage (DS1), moderate damage (DS2), extensive damage (DS3), and complete damage (DS4). Fragility functions for these damage states have already been developed within GEM's new global vulnerability model [13,14], covering more than 900 building classes representative of a broad range of construction materials, structural systems, design-code levels, and ductility classes.

On the contrary, DCR_{DSi} values are rarely available in the literature. The vast majority of studies focused on consequence models associated with economic losses instead [15–18]. This makes it challenging to derive carbon-specific vulnerability functions without relying on simplifications like the use of economic loss ratio as a proxy for its embodied carbon counterpart. While practical, such assumption may lead to overestimating embodied carbon of seismic damage. This is due to the fact that repair costs incorporate contributions that are deemed negligible in the context of carbon footprints, such as labour costs, shoring, formwork, and safety works. These items tend to inflate loss ratios, particularly for lower DSs, where material replacement remains generally limited. Accordingly, to facilitate the derivation of an embodied carbon vulnerability database, reliable DCR_{DSi} values must be developed to be used within Eq. **Error! Reference source not found.**). This is achieved here through the following steps:

1. Select the major (macro) building classes, classified based on their main construction material.
2. Describe the damage observations associated with different DSs for the main structural component (unit) within each major building class.
3. Identify the appropriate repair actions needed to reinstate each damaged structural component to its original condition, depending on the sustained DS.
4. Compute material quantities required to complete each repair action.
5. Multiply material quantities with appropriate ECFs to convert repair action into carbon emissions, which are aggregated for each DS.
6. Emissions associated with each DS are normalised by the embodied carbon of replacing the entire main structural component.

3- DERIVATION OF DAMAGE-TO-CARBON RATIOS

As DCR_{DSi} values must be building-specific, four major building classes are distinguished here based on their primary construction materials as follows: reinforced concrete (CR), steel frames (S), unreinforced masonry (MUR), reinforced masonry (MR), and timber (W) buildings. For each of these major classes, the main structural component is investigated in terms of potential DSs, damage observations, and the required repair actions. All these details are outlined in Table 1 to Table 4, depending on the building class. The information in these tables is obtained from a variety of studies and guidelines looking at building damage [19–24].

Table 1- Damage observations and required repair actions for reinforced concrete structural component

	Major structural component	*Damage observations*	*Repair actions*
DS1	Beam column joint	Minor cracks in the finishing layers, including paint and plastering, covering up to 10% of the structural components outside surface. Additional minor cracks in the attached partitions.	Remove damaged plastering and replace it with a new layer. Repaint the entire external surface of the structural component. Replace the damaged part of the partition.
DS2		Cracks <1.5 mm width at beam-joint interfaces and shear cracks in the joint panel. Additional cracks in beams and column-joint interfaces are expected to form.	Remove external finish (paint and plaster). Clean and inject cracks with epoxy resin. Reconstruct the partitions demolished during the repair process and replaster and repaint repaired areas.
DS3		Existing cracks widen up to 5 mm. Further beam flexural cracks may form. Spalling of concrete cover covering 10% of the joint panel area, with minor bar buckling expected to take place.	Remove external finish (paint and plaster). Clean and inject cracks with epoxy resin. Patch spalled concrete using high-cement mortar. Replace crushed concrete with in-situ mix and replace any buckled steel rebar. Reconstruct the partitions demolished during the repair process and replaster and repaint repaired areas.
DS4		Major spalling occurs, covering at least 40% of the joint panel area with major bar buckling.	Replace the entire component.

Table 2- Damage observations and required repair actions for steel structural component

	Major structural component	*Damage observations*	*Repair actions*
DS1	Beam column joint	Minor damage in the finishing layers and the partitions surrounding the structural component.	Replace the damaged part of the partition and repaint the area.
DS2		Local beam flange and web buckling. Minor damage in the finishing layers and the partitions surrounding the structural component.	Remove external finish (paint and plaster). Clean and inject cracks with epoxy resin. Reconstruct the partitions demolished during the repair process and replaster and repaint repaired areas.
DS3		Lateral torsional distortion in the beam within the hinge region. Damage to the ceiling and surrounding partitions. Major damage in the finishing layers and the partitions surrounding the structural component.	Repair requires the removal and replacement of distorted and/or fractured portion of structural elements. Repair and replace affected partitions at connection and ceiling elements.

DS4		Extensive torsional distortion and the loss of the load-carrying capacity.	Replace the entire structural component.

Table 3- Damage observations and required repair actions for unreinforced masonry structural component

	Major structural component	*Damage observations*	*Repair actions*
DS1	Load-bearing wall	Light diagonal cracking in the finishing layer (paint and plastering).	Demolish cracked plastering and replace it with a new one, followed by repainting the entire wall.
DS2		Extended cracking and potential failure of some brick units.	Remove damaged brick units and build new ones. Demolish cracked plastering and replace it with a new one, followed by repainting the entire wall.
DS3		Extended brick failure. Buckling in some steel rebar within the wall (only for reinforced masonry).	Remove damaged brick units and build new ones. Demolish cracked plastering and replace it with a new one, followed by repainting the entire wall. Also replace buckled bars and their surrounding mortar (for reinforced masonry only).
DS4		Severe brick failure and bar buckling. Wall is deemed irreparable.	Replace the entire component.

Table 4- Damage observations and required repair actions for timber structural component

	Major structural component	*Damage observations*	*Repair actions*
DS1	Light framed wood walls with structural panel sheathing and gypsum plasterboard	Slight separation of sheathing or nails, which become loose.	Remove exterior siding (cladding), replace loose nails, and reinstall siding. Repaint and replaster in the area where works took place.
DS2		Permanent rotation in some areas of the sheathing, in addition to tearing out for nails or parts of the sheathing.	Remove exterior siding (cladding) and then replace the entire structural sheathing layer. Repaint and replaster in the area where works took place.
DS3		Fracture of studs, major plate cracking.	Remove and replace damaged parts of siding, studs and plates. Remove and replace sheathing. Replace the gypsum drywall and then repaint and replaster.
DS4		Extensive failure and loss of load-carrying capacity.	Replace the entire component.

Once the repair actions corresponding to each DS are identified for the main structural components, it is possible to compute the required material quantities. To account for the geometric variability of these components, a Monte Carlo sampling approach is adopted. For example, masonry walls and timber units are assumed to have widths ranging from 3.5 to 5.0 m and heights between 2.2 and 3.0 m. In reinforced concrete joints, beam widths and depths vary between 0.3 and 0.4 m and 0.4 and 0.6 m, respectively, while column dimensions range from 0.4 to 0.6 m. For steel joints, a range of I-sections is considered for beams, from W24x55 to W27x146, and for columns, from W12x87 to W14x193. Based on these assumptions, 100,000 geometric combinations are simulated by sampling the geometric parameters from uniform distributions [16,24]. For steel beams and columns, the section size is randomly selected from the predefined pool, while ensuring that the flange width of the column section is greater than that of the beam section to satisfy constructability requirements.

The estimated material quantities can now be converted to embodied carbon by multiplying them with the appropriate ECF values. ECFs represent the carbon emissions per unit quantities (e.g., tonne, kg, m^2, m^3)

associated with the production process of construction materials (namely, modules A1-A3 in the life-cycle stages [25]). These factors can be obtained from several databases, such as the Inventory of Carbon and Energy (ICE) [26] and the Embodied Carbon in Construction Calculator (EC3) [27]. In this study, we use the open-access database created by Caruso et al. [12], which compiles European carbon data for a broad range of materials and structural and non-structural components. The database brings together information from published studies, existing datasets, and technical guidelines. For illustration purposes, a sample of the adopted ECF values is presented in **Error! Reference source not found.** reported in terms of mean values and coefficients of variation.

Table 5- Embodied carbon factors (ECFs) for selected materials; adapted from [12]

	Average ECF (kg CO_2e/unit)	*Unit*	*Coefficient of variation*
Steel rebars	0.87	kg	0.60
Ready-mix concrete	271.00	m^3	0.21
Structural mass timber	162.00	m^3	0.64
Clay bricks	0.20	kg	0.40
Hot-rolled steel sections	0.69	kg	0.35
Sand	63.32	tonne	0.33
Cold formed steel	2.52	kg	0.22
Cement	789.00	tonne	0.18

It should be noted that the variability of ECF values is also addressed while computing the embodied carbon due to repair activities. This is achieved by generating samples from the average and coefficient of variation values in **Error! Reference source not found.** via Monte Carlo simulations before multiplying the resulting samples with the corresponding material quantities. The effects of de-construction, demolition, waste processing, and disposal prior to repair works are considered separately using the simplified procedure described in Aljawhari et al. [9] and then added to the computed embodied carbon values.

Finally, the resulting embodied carbon realisations are aggregated for each structural component and for each DS and then divided by the replacement embodied carbon to generate the DCR_{DSi} values, expressed as median values and dispersions. Figure 1 depicts the resulting median DCR_{DSi} values, considering the four DSs and the four major building classes defined earlier. The exact values of these medians, in addition to the computed dispersion, are outlined in Table 6.

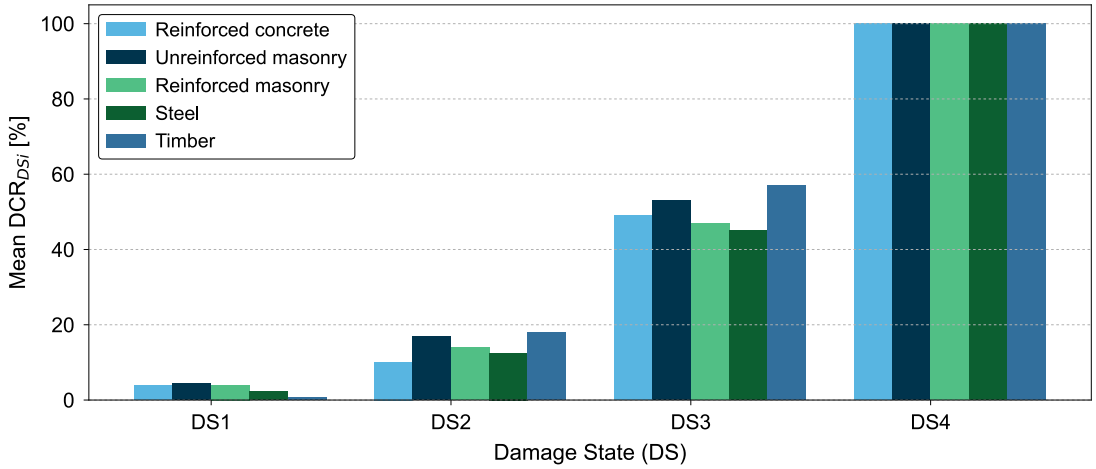


Figure 1- The derived DCR_{DSi} values for the major building classes

Table 6- Damage-to-carbon ratios (DCR_{DSi}) for the major building classes

	DCR_{DS1}		DCR_{DS2}		DCR_{DS3}		DCR_{DS4}	
	Medi	Dispersion	Median	Dispersion	Median	Dispersion	Median	Dispersion
Reinforced concrete	3.80%	0.15	10.10%	0.13	49.00%	0.15	100%	N.A.
Steel	2.30%	0.22	12.50%	0.24	45.00%	0.20	100%	N.A.

Unreinforc-ed Masonry	4.30%	0.17	16.90%	0.15	53.00%	0.21	100%	N.A.
Reinforced Masonry	4.00%	0.16	13.90%	0.13	46.00%	0.18	100%	N.A.
Timber	0.73%	0.24	18.00%	0.44	57.00%	0.19	100%	N.A.

As shown by Figure 1 and Table 6, the median DCR_{DSi} values vary substantially across the four major building classes, particularly at the lower levels of damage (i.e., DS1 and DS2). For example, the median DCR_{DS1} can be as small as 0.73% for timber structures and reaches up to 4.3% for unreinforced masonry. For DS2 and DS3, the median DCR_{DSi} values are relatively similar for the reinforced concrete, masonry, and steel buildings, whereas noticeably higher values are observed for timber structures. For DS4, the DCR_{DSi} values are assumed equal to 100% as they involve the complete replacement of the structural component.

These results indicate clearly that it important to use structure-specific DCR_{DSi} values, at least at the level of the main construction material of the building. It is acknowledged that a finer level of accuracy can be achieved by distinguishing among different structural systems within each construction material, however, the adopted level of resolution remains appropriate for regional seismic risk applications. In fact, most large-scale assessments still rely on vulnerability functions derived from a single set of damage-to-loss ratios, without accounting for building-specific characteristics [13,28,29].

4- EMBODIED CARBON VULNERABILITY FUNCTIONS

Upon deriving DCR_{DSi} values for the four major building classes (reinforced concrete, unreinforced masonry, reinforced masonry, steel, and timber), they are combined with fragility functions via Eq. (1) to generate the required carbon-specific vulnerability functions. The required fragility functions have been derived in a previous study by Aljawhari et al. [13] within the scope of GEM's Global Vulnerability Model [13,14]. They address more than 900 building classes, spanning a wide range of construction materials, structural systems, heights, design codes, and ductility levels. Each building class is identified using a string that combines the previous attributes following GEM's taxonomy [30]. For example, CR/LFM+CDM+DUL/H:2/RES represents a two-storey (H:2) reinforced concrete (CR) moment-resisting frame (LFM) with moderate code design (CDM), low ductility (DUL), and residential (RES) occupancy. Further information on all building classes and their global distribution is provided in Yepes-Estrada et al. [31].

The resulting vulnerability functions are available on our GitHub [1] repository. Sample functions are shown in Figure 2 for these building classes: a) three-storey reinforced concrete dual frame with high code and ductility class (CR/LDUAL+CDH+DUH/H:3); b) 10-storey reinforced concrete bare frame with low code and ductility class (CR/LFM+CDL+DUL/H:10); c) two-storey timber frame with low ductility (W/LFM+CDL/H:2); and d) one-storey steel braced frame with moderate code and ductility (S/LFBR+CDM+DUM/H:1). For comparison, Figure 2 also shows both the embodied carbon vulnerability (dashed lines) and the corresponding economic loss vulnerability functions (solid lines). The latter are based on the typical damage-to-loss ratios of 5%, 20%, 60%, and 100% for DS1 to DS4, respectively [28].

Figure 2 clearly shows that the economic loss ratio is consistently higher than its embodied carbon counterpart across all IM levels and for all four building classes. This trend is primarily explained by the fact that the derived DCR_{DS_i} values, except for DS4, are generally lower than the corresponding conventional damage-to-loss ratios. This is especially pronounced at low IM levels, where lower DSs, such as DS1 and DS2, are more likely to occur. At these IM levels, the economic loss ratio can exceed the embodied carbon ratio by more than 200%, as observed, for example, for the S/LFBR+CDM+DUM/H:1 building class in Figure 2(d). A similar pattern is found for the W/LFM+CDL/H:2 building class, for which the DCR_{DS1} value is substantially lower than the corresponding damage-to-loss ratio.

It is also important to highlight the influence of seismic performance, governed by design-code level and ductility, on the difference between embodied carbon and economic loss vulnerability functions. For instance, the vulnerability functions for the CR/LDUAL+CDH+DUH/H:3 and CR/LFM+CDL+DUL/H:10 building classes shown in Figure 2 (a–b) are derived using the same DCR_{DS_i} values and the same conventional damage-to-loss ratios. However, while the functions in the latter case are nearly identical, the differences are much more pronounced in the former case. This is because the CR/LFM+CDL+DUL/H:10 class, characterised by low code and low ductility, is dominated by higher DSs, namely DS3 and DS4, for which the DCR_{DS_i} values and economic damage-to-loss ratios are relatively close in the case of DS3 and identical in the case of DS4.

[1] https://github.com/gem/global_vulnerability_model

Overall, this indicates that the divergence between embodied carbon and economic loss vulnerability functions tends to be greater for buildings with better seismic performance.

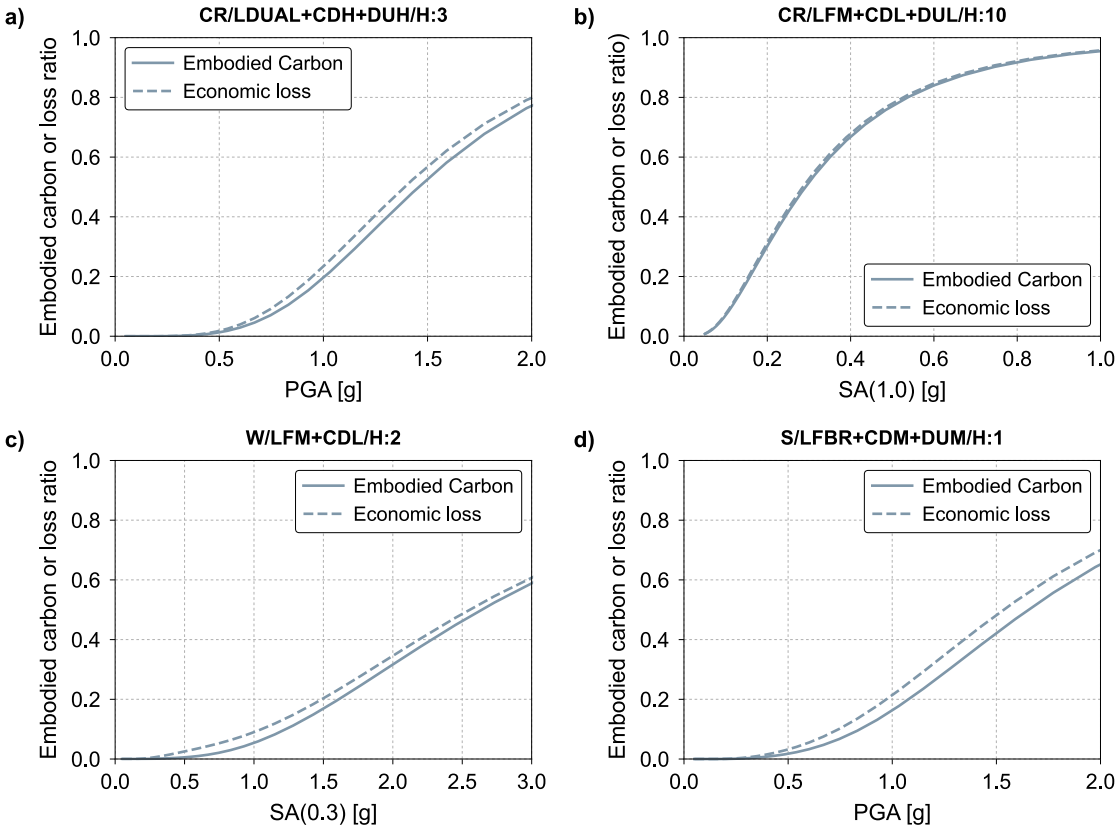


Figure 2- Embodied carbon and economic loss vulnerability functions derived for the following building classes: a) three-storey reinforced concrete dual frame with high code and ductility class; b) 10-storey reinforced concrete bare frame with low code and ductility class; c) two-storey timber frame with low ductility; and d) one-storey steel braced frame with moderate code and ductility

5- CONCLUSIONS

This study introduced a carbon-specific structural vulnerability database for Europe, developed to improve the estimation of earthquake-induced embodied carbon losses at large scale. The study addressed a key limitation in previous regional assessments, where embodied carbon losses were approximated using conventional economic vulnerability functions. The results demonstrate that this assumption can significantly overestimate environmental losses, especially at low shaking intensities.

A new set of carbon-specific damage-to-carbon ratios, DCR_{DS_i}, was developed for four major building classes: reinforced concrete, reinforced and unreinforced masonry, steel, and timber. These were obtained by identifying damage-state-specific repair actions, estimating the corresponding material quantities through Monte Carlo simulation, and converting them into embodied carbon using European embodied carbon factors, ECFs. By combining these consequence models with fragility functions from GEM's Global Vulnerability Model, embodied carbon vulnerability functions were generated for more than 900 building classes.

The derived DCR_{DS_i} values showed clear differences across building classes, particularly at lower DSs, confirming that embodied carbon losses should not be represented using generic or cost-based loss ratios. The resulting vulnerability functions were consistently lower than their economic counterparts, with the largest discrepancies observed at lower IM levels. In some cases, economic loss ratios exceeded embodied carbon ratios by more than twice, indicating that cost-based proxies may lead to bias in carbon-based risk estimates.

The proposed database therefore provides a more robust and physically meaningful basis for regional and continental assessments of earthquake-induced embodied carbon.

Future developments shall address the embodied-carbon contribution associated with the damage and subsequent repair works for non-structural building components, which typically constitute the largest share of carbon footprints [12] and costs [31] related to construction.

6- REFERENCES

[1] Gonzalez RE, Stephens MT, Toma C, Dowdell D. The Estimated Carbon Cost of Concrete Building Demolitions following the Canterbury Earthquake Sequence. Earthquake Spectra 2022;38:1615–35. https://doi.org/10.1177/87552930221082684.

[2] Bektaş N, Jingjie Z. Sustainable waste management strategies for earthquake debris: Lessons from the 2008 China and 2023 Türkiye-Syria disasters. International Journal of Disaster Risk Reduction 2025;116:105153. https://doi.org/10.1016/j.ijdrr.2024.105153.

[3] D&R International. 2011 Building Energy Data Book, The U.S. Department of Energy. Silver Spring; 2012.

[4] Belleri A, Marini A. Does seismic risk affect the environmental impact of existing buildings? Energy Build 2016;110:149–58. https://doi.org/10.1016/j.enbuild.2015.10.048.

[5] Pajgade RP, Raghunandan M, Ghosh S. An integrated life cycle cost assessment framework incorporating cost of carbon dioxide equivalent for buildings subjected to natural hazards. Sustain Cities Soc 2025;126:106394. https://doi.org/10.1016/j.scs.2025.106394.

[6] Aljawhari K, Gentile R, Galasso C. Beyond Direct Economic Losses: An Integrated Approach to Seismic Retrofit Considering Sustainability and Indirect Losses. Earthq Eng Struct Dyn 2025. https://doi.org/10.1002/eqe.4324.

[7] Caruso M, Couto R, Pinho R, Monteiro R. Decision-making approaches for optimal seismic/energy integrated retrofitting of existing buildings. Front Built Environ 2023;9. https://doi.org/10.3389/fbuil.2023.1176515.

[8] Caruso M, Pinho R, Bianchi F, Cavalieri F, Lemmo MT. Multi-criteria decision-making approach for optimal seismic/energy retrofitting of existing buildings. Earthquake Spectra 2023;39:191–217. https://doi.org/10.1177/87552930221141917.

[9] Aljawhari K, Gentile R, Galasso C. Earthquake-induced Environmental Impacts for Residential Italian Buildings: Consequence Models and Risk Assessment. Journal of Building Engineering 2023. https://doi.org/doi.org/10.1016/j.jobe.2023.108149.

[10] Anwar GA, Dong Y, Zhai C. Performance-based probabilistic framework for seismic risk, resilience, and sustainability assessment of reinforced concrete structures. Advances in Structural Engineering 2020;23:1454–72. https://doi.org/10.1177/1369433219895363.

[11] Chiu CK, Chen MR, Chiu CH. Financial and Environmental Payback Periods of Seismic Retrofit Investments for Reinforced Concrete Buildings Estimated Using a Novel Method. Journal of Architectural Engineering 2013;19:112–8. https://doi.org/10.1061/(asce)ae.1943-5568.0000105.

[12] Caruso M, Silva V, Aljawhari K, Nafeh AMB, Galasso C. Unveiling the environmental impact of earthquakes in Europe. Nat Commun 2026;17:1366. https://doi.org/10.1038/s41467-025-68120-6.

[13] Aljawhari K, Nafeh AMB, Silva V. A New Global Vulnerability Model for Regional Seismic Risk Assessments: Part 1 – Structural Vulnerability. Bulletin of Earthquake Engineering 2026. https://doi.org/10.1007/s10518-026-02443-7.

[14] Nafeh AMB, Aljawhari K, Silva V. A New Global Vulnerability Model for Regional Seismic Risk Assessments: Part 2 – Non-structural and Building Content Vulnerability. Bulletin of Earthquake Engineering (Under Review) 2026.

[15] Martins L, Silva V, Marques M, Crowley H, Delgado R. Development and assessment of damage-to-loss models for moment-frame reinforced concrete buildings. Earthq Eng Struct Dyn 2016;45:797–817. https://doi.org/10.1002/eqe.2687.

[16] Aljawhari K, Gentile R, Galasso C. Simulation-based consequence models of seismic direct loss and repair time for archetype reinforced concrete frames. Soil Dynamics and Earthquake Engineering 2023;172:107979. https://doi.org/10.1016/j.soildyn.2023.107979.

[17] Bal IE, Crowley H, Pinho R, Gülay FG. Detailed assessment of structural characteristics of Turkish RC building stock for loss assessment models. Soil Dynamics and Earthquake Engineering 2008;28:914–32. https://doi.org/10.1016/j.soildyn.2007.10.005.

[18] Di Pasquale G, Orsini G, Romeo RW. New developments in seismic risk assessment in Italy. Bulletin of Earthquake Engineering 2005;3:101–28. https://doi.org/10.1007/s10518-005-0202-1.

[19] Cardone D, Perrone G. Damage and Loss Assessment of Pre-70 RC Frame Buildings with FEMA P-58. Journal of Earthquake Engineering 2017;21:23–61. https://doi.org/10.1080/13632469.2016.1149893.
[20] Applied Technology Council. Seismic Performance Assessment of Buildings. Fema P-58-5 2018;2.
[21] Cardone D, Perrone G. Developing fragility curves and loss functions for masonry infill walls. Earthquake and Structures 2015;9:257–79. https://doi.org/10.12989/eas.2015.9.1.257.
[22] Cardone D. Fragility curves and loss functions for RC structural components with smooth rebars. Earthquake and Structures 2016;10:1181–212. https://doi.org/10.12989/eas.2016.10.5.1181.
[23] Ottonelli D, Cattari S, Lagomarsino S. Displacement-Based Simplified Seismic Loss Assessment of Masonry Buildings. Journal of Earthquake Engineering 2020;24:23–59. https://doi.org/10.1080/13632469.2020.1755747.
[24] De Risi MT, Del Gaudio C, Verderame GM. A component-level methodology to evaluate the seismic repair costs of infills and services for Italian RC buildings. vol. 18. Springer Netherlands; 2020. https://doi.org/10.1007/s10518-020-00944-7.
[25] EN 15804. Sustainability of construction works. Environmental product declarations. Core rules for the product category of construction products. 2012.
[26] Hammond GP, Jones CI. Embodied energy and carbon in construction materials. Proceedings of Institution of Civil Engineers: Energy 2008;161:87–98. https://doi.org/10.1680/ener.2008.161.2.87.
[27] Building Transparancy. Embodied Carbon in Construction Calculator (EC3) Tool. Https://BuildingtransparencyOrg/Ec3 2024.
[28] Martins L, Silva V. Development of a fragility and vulnerability model for global seismic risk analyses. Bulletin of Earthquake Engineering 2021;19:6719–45. https://doi.org/10.1007/s10518-020-00885-1.
[29] FEMA. Hazus Earthquake Model Technical Manual. Federal Emergency Management Agency 2020:1–436.
[30] Silva V, Brzev S, Scawthorn C, Yepes C, Dabbeek J, Crowley H. A Building Classification System for Multi-hazard Risk Assessment. International Journal of Disaster Risk Science 2022;13:161–77. https://doi.org/10.1007/s13753-022-00400-x.
[31] Yepes-Estrada C, Calderon A, Costa C, Crowley H, Dabbeek J, Hoyos MC, et al. Global building exposure model for earthquake risk assessment. Earthquake Spectra 2023;39:2212–35. https://doi.org/10.1177/87552930231194048.